Modulation of $Ca_V1.2$ Channels by Mg^{2+} Acting at an EF-hand Motif in the COOH-terminal Domain

Sylvain Brunet,[1] Todd Scheuer,[1] Rachel Klevit,[2] and William A. Catterall[1]

[1]Department of Pharmacology and [2]Department of Biochemistry, University of Washington, Seattle, WA 98195

Magnesium levels in cardiac myocytes change in cardiovascular diseases. Intracellular free magnesium (Mg_i) inhibits L-type Ca^{2+} currents through $Ca_V1.2$ channels in cardiac myocytes, but the mechanism of this effect is unknown. We hypothesized that Mg_i acts through the COOH-terminal EF-hand of $Ca_V1.2$. EF-hand mutants were engineered to have either decreased (D1546A/N/S/K) or increased (K1543D and K1539D) Mg^{2+} affinity. In whole-cell patch clamp experiments, increased Mg_i reduced both Ba^{2+} and Ca^{2+} currents conducted by wild type (WT) $Ca_V1.2$ channels expressed in tsA-201 cells with similar affinity. Exposure of WT $Ca_V1.2$ to lower Mg_i (0.26 mM) increased the amplitudes of Ba^{2+} currents 2.6 ± 0.4–fold without effects on the voltage dependence of activation and inactivation. In contrast, increasing Mg_i to 2.4 or 7.2 mM reduced current amplitude to 0.5 ± 0.1 and 0.26 ± 0.05 of the control level at 0.8 mM Mg_i. The effects of Mg_i on peak Ba^{2+} currents were approximately fit by a single binding site model with an apparent K_d of 0.65 mM. The apparent K_d for this effect of Mg_i was shifted ~3.3- to 16.5-fold to higher concentration in D1546A/N/S mutants, with only small effects on the voltage dependence of activation and inactivation. Moreover, mutant D1546K was insensitive to Mg_i up to 7.2 mM. In contrast to these results, peak Ba^{2+} currents through the K1543D mutant were inhibited by lower concentrations of Mg_i compared with WT, consistent with approximately fourfold reduction in apparent K_d for Mg_i, and inhibition of mutant K1539D by Mg_i was also increased comparably. In addition to these effects, voltage-dependent inactivation of K1543D and K1539D was incomplete at positive membrane potentials when Mg_i was reduced to 0.26 or 0.1 mM, respectively. These results support a novel mechanism linking the COOH-terminal EF-hand with modulation of $Ca_V1.2$ channels by Mg_i. Our findings expand the repertoire of modulatory interactions taking place at the COOH terminus of $Ca_V1.2$ channels, and reveal a potentially important role of Mg_i binding to the COOH-terminal EF-hand in regulating Ca^{2+} influx in physiological and pathophysiological states.

The Journal of General Physiology

INTRODUCTION

Magnesium is the second most abundant intracellular cation (Elin, 1994). In the heart, the level of free intracellular magnesium (Mg_i) is well controlled but alterations are observed in a variety of cardiovascular diseases (Murphy, 2000). For example, during myocardial ischemia, there is a reciprocal relationship between decreased ATP and increased Mg_i levels, and Mg_i rises 3.5-fold as ATP levels fall (Murphy et al., 1989). Cardiovascular diseases are associated with alterations in Ca^{2+} homeostasis (Tomaselli and Marban, 1999), and Mg_i can modulate multiple proteins involved in Ca^{2+} transport (White and Hartzell, 1988, 1989; Hartzell and White, 1989; Xu et al., 1996; Wei et al., 2002), including substantial effects on the L-type Ca^{2+} current density, inactivation, and voltage dependence (White and Hartzell, 1988; Agus et al., 1989; Kuo and Hess, 1993; Yamaoka and Seyama, 1996; Pelzer et al., 2001; Wang et al., 2004). The molecular mechanisms responsible for these modulatory effects of Mg_i on L-type Ca^{2+} currents are unknown. It has been proposed that Mg_i could produce its effects directly by interacting with the Ca^{2+} channel protein (Kuo and Hess, 1993; Yamaoka and Seyama, 1996) or indirectly by altering enzyme activities that require Mg_i as a cofactor or regulator, such as protein kinases or phosphoprotein phosphatases (Pelzer et al., 2001).

In ventricular myocytes, L-type Ca^{2+} currents are conducted by $Ca_V1.2$ channels consisting of a pore-forming $\alpha_1 1.2$ subunit in association with β and α2δ subunits (Catterall, 2000). The α1 subunits are composed of four homologous domains (I–IV) with six transmembrane segments (S1–S6) and a reentrant pore loop in each. Regulatory sites for Ca^{2+}/calmodulin and cAMP-dependent protein kinase are located in the COOH-terminal domain (De Jongh et al., 1996; Peterson et al., 1999; Zuhlke et al., 1999; Hulme et al., 2003), which is also subject to in vivo proteolytic processing (De Jongh et al., 1991, 1996). The COOH-terminal domain contains an EF-hand motif that is expected to bind divalent cations (de Leon et al., 1995). Studies of Ca^{2+} channel chimeras suggested a role for the EF-hand in Ca^{2+}-dependent inactivation

Correspondence to William A. Catterall: wcatt@u.washington.edu

The online version of this article contains supplemental material.

Abbreviations used in this paper: Mg_i, intracellular free magnesium; WT, wild-type.

(de Leon et al., 1995), but mutations in the amino acid residues that are required for divalent cation binding have no effect on inactivation (Zhou et al., 1997; Peterson et al., 2000), indicating that the role of the EF-hand in Ca^{2+}-dependent inactivation is structural. A nearby IQ domain is directly implicated in Ca^{2+}-dependent inactivation mediated by Ca^{2+}/calmodulin (Peterson et al., 1999; Zuhlke et al., 1999), and structural changes in the EF-hand may impair the inactivation process indirectly.

Could the COOH-terminal EF-hand motif of $Ca_V1.2$ channels be involved in modulation by Mg_i? EF-hands are composed of a helix-loop-helix motif, where the loop of 12 amino acid residues forms the cation-binding site (Kawasaki and Kretsinger, 1994). In addition to Ca^{2+}, Mg^{2+} at physiological concentrations can bind to some EF-hand motifs with appropriate amino acid sequences (da Silva et al., 1995; Houdusse and Cohen, 1996; Lewit-Bentley and Rety, 2000; Yang et al., 2002). Inspection of the amino acid sequence of the $Ca_V1.2$ COOH-terminal EF-hand suggested that it could bind Mg_i. Therefore, we constructed EF-hand ion-coordination site mutants and compared their electrophysiological properties with wild-type (WT) $Ca_V1.2$ channels. Our results support a novel mechanism linking the COOH-terminal EF-hand motif of $Ca_V1.2$ with the modulation of $Ca_V1.2$ channels by intracellular Mg^{2+} (Brunet et al., 2004). These findings expand the repertoire of modulatory interactions that take place at the COOH terminus of $Ca_V1.2$ channels and suggest that Mg_i bound to the COOH-terminal EF-hand may have an important role in regulating Ca^{2+} influx in physiological and pathophysiological states.

MATERIALS AND METHODS

Cell Culture and Expression

TsA-201 cells, a subclone of the human embryonic kidney cell line HEK-293 that expresses the simian virus 40 T-antigen (a gift of Robert Dubridge, Cell Genesis, Foster City, CA), were grown in DMEM/Ham's F-12 medium (Life Technologies), supplemented with 10% (vol/vol) FBS (Hyclone), and incubated at 37°C in 10% CO_2. TsA-201 cells were grown to 80% confluence, suspended with trypsin/EDTA, and plated onto 35-mm culture dishes (Corning) at 40% confluence 24 h before transfection. Immediately before transfection, the medium was replaced with fresh DMEM/F-12 supplemented with serum and antibiotics, and the cells were transiently transfected with cDNA encoding rabbit cardiac $Ca_V1.2$, β_{1b}, and $\alpha2\delta$ subunits at 1:1:1 molar ratio by using the Ca^{2+} phosphate method or the Fugene method (Invitrogen) in accordance with the manufacturer's protocol. In addition, a 10-fold lower molar concentration of cDNA encoding CD-8 antigen (EBO-pCD-Leu2; American Type Culture Collection) was added to each transfection. The cells were incubated overnight at 37°C in 3% CO_2. For Ca^{2+} phosphate transfection, the medium was replaced with fresh DMEM/F12 after 6–7 h, and the cells were allowed to recover for 15 h. For Fugene transfection, the cells were incubated with Fugene for 24 h at 3% CO_2. After recovering from transfection for 15 h or 24 h, the cells were suspended using EDTA, plated in 35-mm dishes, and incubated at 37°C in 10% CO_2 for at least 3–4 h before recording.

Electrophysiological Recordings

Immediately before recording, a 35-mm culture dish with transfected cells was stirred for 1 min with latex beads conjugated to an anti-CD8 antibody (Dynal), which bound those cells that had been successfully transfected with the Ca^{2+} channels plus CD-8 receptor (Margolskee et al., 1993). The extracellular recording solution contained (in mM) 10 $BaCl_2$, 140 Tris, 2 $MgCl_2$, and 10 D-glucose titrated to pH 7.3 with $MeSO_4H$. For some recordings, 1.8 mM $CaCl_2$ was substituted for 10 mM $BaCl_2$ with appropriate adjustment of osmolarity. The control intracellular Mg^{2+} (0.8 mM free Mg^{2+}) solution contained (in mM) 130 *N*-methyl-D-glucamine, 60 Hepes, 5 MgATP, 1 $MgCl_2$, and 10 EGTA titrated to pH 7.3 with $MeSO_4H$. The osmolarity of all solutions was adjusted to 295 mOsM with sucrose. The free intracellular Mg^{2+} concentration was altered by changing the $MgCl_2$ in the intracellular solution. Free $[Mg^{2+}]_i$ was calculated by Maxchelator program (Bers et al., 1994).

Voltage clamp recordings were made in the whole-cell configuration using an Axopatch 200A amplifier (Axon Instruments). Linear leak and capacitance were cancelled using the internal amplifier circuitry and >80% of the series resistance was compensated. Pipettes were pulled from VWR micropipettes. After achieving the whole cell configuration, pipette resistances were from 2 to 5 MΩ. The design of this study required recording currents with a broad range of magnitudes under identical conditions. To avoid poor voltage control for cells with large currents, larger pipettes were used in combination with maximal series resistance compensation. Voltage clamp fidelity was assessed for each cell and cells with >5 mV uncompensated voltage error, steep current–voltage relationships, and/or slowly decaying tail currents were omitted from analysis.

Construction of EF-hand Mutants

To construct mutants D1546A/N/S/K, K1539D, and K1543D, mutagenic primers were designed that contained an internal HindIII restriction site. K1539D, K1543D, and D1546A/N/S/K were all amplified in a two-phase manner, using a SacII-XhoI cDNA fragment of $Ca_V1.2$ in pBluescript SK+. Phase I generated the 5′ and the 3′ arms using the WT DNA template. PCR products were gel purified. Phase II combined the 5′ and 3′ arms to serve as both initial primers and template. PCR products were precipitated, washed, dried, and resuspended. PCR products and vector were cut with Sac II and Xho I and isolated by ethanol precipitation. The digested vector was treated with calf alkaline phosphatase (CIP, NEB). Digested DNA was run out on a 1.25% agarose gel. Fragment bands were excised and purified either by Spin-X column (Fisher Scientific) or QIAQuick (QIAGEN). Fragments were ligated (Fast-Link, Epicentre). A negative control of vector and no insert was run at the same time. Ligation mixtures were then transformed into competent DH5 cells and samples were plated onto LB plates overnight. DNA was extracted from mutant colonies by basic SDS/sodium acetate method. Samples were screened by cutting with restriction enzymes whose recognition sites were silently built into the mutation primer. Positive samples were further purified (Quantum miniprep kit, Bio-Rad Laboratories) and sequenced (BigDye, ABI). When the sequences were confirmed to be correct, DNA from the original mini-prep was retransformed, amplified, and extracted (QUANTUM maxiprep kit, Bio-Rad Laboratories). Each mutant DNA in pBluescript SK+ (Stratagene) and the full-length WT $Ca_V1.2$ α in pCDNA3 (Stratagene) were digested with Sac II and Xho I, ligated, and subcloned. Samples were sequenced again to confirm the sequence of the final construct.

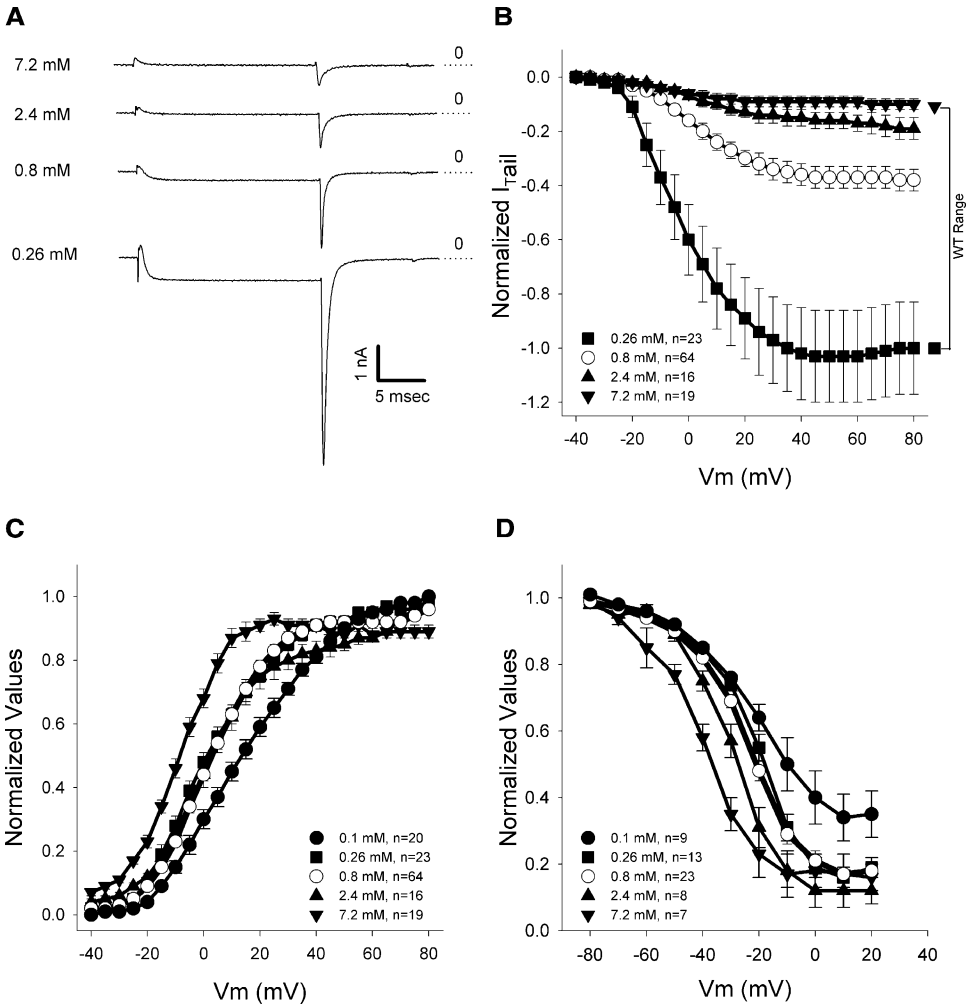

Figure 1. Effect of Mg_i on $Ca_V1.2$ channels. (A) Typical current traces from cells exposed to the indicated concentrations of Mg_i. Ba^{2+} currents were elicited by a depolarization to +40 mV. (B) Effect of Mg_i on normalized tail current amplitudes (mean I_{tail}/mean I_{tail} [0.26 mM Mg_i]). Under voltage clamp conditions, Ba^{2+} currents were elicited by a 20-ms depolarization from a holding potential of −80 mV to potentials from −40 to 80 mV in 5-mV increments followed by a step repolarization to −40 mV to elicit tail currents. The bracket labeled WT Range indicates the change in normalized tail current amplitude for a change from 0.26 mM to 7.2 mM Mg_i. (C) Effect of Mg_i on the voltage dependence of activation of $Ca_V1.2$ channels. Tail current amplitudes were normalized to the maximum value at positive test potential. (D) Effect of Mg_i on the voltage dependence of inactivation of $Ca_V1.2$ channels. Under voltage clamp conditions, tsA-201 cells were depolarized from a holding potential of −80 mV for 4 s to membrane potentials from −80 to 20 mV in 10-mV increments. Ba^{2+} currents were then elicited by depolarization to 30 mV for 30 ms, followed by repolarization to −40 mV to measure tail currents.

Data Analysis

Voltage-clamp data were compiled and analyzed using Igor (IGOR Pro version 5.0, Wavemetrics Inc.) and Excel (Excel 97, Microsoft). Peak tail currents were measured during repolarization to −40 mV after a 20-ms depolarization to potentials between −40 and 80 mV. For the measurement of the voltage dependence of inactivation, 4-s depolarizations to potentials from −80 to 20 mV were applied to inactivate a fraction of $Ca_v1.2$ channels. A standard test pulse of 30 ms to 30 mV was applied, and peak tail currents were measured during repolarization to −40 mV immediately following the test pulse. To control for differences in expression levels between transfections, individual cells recorded with control Mg_i (0.8 mM Mg_i) were alternated with cells recorded at test Mg_i concentrations during each recording period. Activation and inactivation data were fit to a Boltzmann function (Sigmaplot version 7.0, Systat Software). Differences between control and experimental values were assessed using ANOVA and the Student's t test; P values <0.05 were considered statistically significant.

Online Supplemental Material

The mean values for all of the parameters describing the voltage dependence of activation and inactivation for WT $Ca_V1.2$ and EF-hand mutants are presented in Table S1 (available at http://www.jgp.org/cgi/content/full/jgp.200509333/DC1).

RESULTS

Modulation of $Ca_V1.2$ Channels by Intracellular Mg^{2+}

To determine whether Mg_i modulates cloned $Ca_V1.2$ channels expressed in tsA-201 cells, we examined the electrophysiological properties of WT $Ca_V1.2$ channels over a range of intracellular Mg_i concentrations from 0.1 to 7.2 mM. Changes in Mg_i in this range modulated the peak current amplitude in all cases and altered the voltage dependence of activation and inactivation at the extreme concentrations. We were unable to study lower intracellular Mg^{2+} concentrations because the recordings became unstable. Higher intracellular Mg^{2+} concentrations depressed the Ba^{2+} current too much for accurate measurements. As each measurement was necessarily made on a separate cell, we interleaved cells at 0.8 mM Mg_i and other test concentrations to be certain that no artifactual drift in electrophysiological parameters occurred during a recording period. The principal experimental results are presented in the figures and text below, whereas mean values for all of the parameters de-

scribing the voltage dependence of activation and inactivation are presented in Table S1 (available at http://www.jgp.org/cgi/content/full/jgp.200509333/DC1).

Changes in Mg_i modulated the peak Ba^{2+} current conducted by $Ca_V1.2$ channels (Fig. 1 A). Reduction in Mg_i from the control level of 0.8 mM increased Ba^{2+} current, and increases in Mg_i decreased Ba^{2+} current. Parallel changes were observed in the amplitudes of tail currents recorded after repolarization to −40 mV (Fig. 1 A). We used the tail currents as a measure of Ba^{2+} conductance to analyze inhibition by Mg_i at different test pulse potentials as well as to determine the voltage dependence of activation and inactivation. In the presence of the 0.8 mM Mg_i, the tail current first was observed at −25 mV, increased progressively with more depolarized test potentials, and reached a plateau at potentials more positive than +30 mV (Fig. 1, A and B). Higher concentrations of Mg_i significantly reduced tail current amplitude across the entire voltage range, while lower Mg_i significantly increased it (Fig. 1, A and B). Thus, increases in Mg_i cause primarily voltage-independent inhibition of peak Ba^{2+} currents through $Ca_V1.2$ channels.

Effects of Mg_i on the voltage dependence of activation and inactivation were observed at the highest and lowest Mg_i concentrations tested. The highest Mg_i tested (7.2 mM) led to a shift of −7.5 mV in the activation curve (Fig. 1 C), while reducing Mg_i to 0.1 mM shifted the activation curve by +10.1 mV (Fig. 1 C). In contrast, changes in Mg_i between 0.26 and 2.4 mM did not cause changes in the voltage dependence of activation (Fig. 1 C and Table S1). High Mg_i concentrations (2.4 and 7.2 mM) also caused negative shifts (−5 and −10 mV, respectively) of the voltage dependence of inactivation (Fig. 1 D), whereas lower Mg_i did not alter the voltage dependence of inactivation but made inactivation incomplete (Fig. 1 D).

Concentration-dependent Inhibition of Ba^{2+} and Ca^{2+} Currents by Mg_i

Although changes in Mg_i caused shifts in the voltage dependence of both activation and inactivation, peak Ba^{2+} currents reached a plateau at voltages more positive than 30 mV for all Mg_i concentrations (Fig. 1 B). Therefore, the reductions of peak Ba^{2+} current with increasing Mg_i at test potentials more positive than 30 mV were readily separated from effects on voltage dependence. The requirement to measure Ba^{2+} currents at different Mg_i concentrations in separate cells introduced variability due to the different expression levels of Ca^{2+} channels among cells. Despite this variability, we found that the mean values for peak Ba^{2+} currents were significantly different as a function of Mg_i, and could be approximated by a single binding isotherm with an apparent K_d value of 0.65 mM (Fig. 2 A). Although the fit to a single binding site model is only approximate, a one-site model was significantly better than a fit to a two binding site model in a glo-

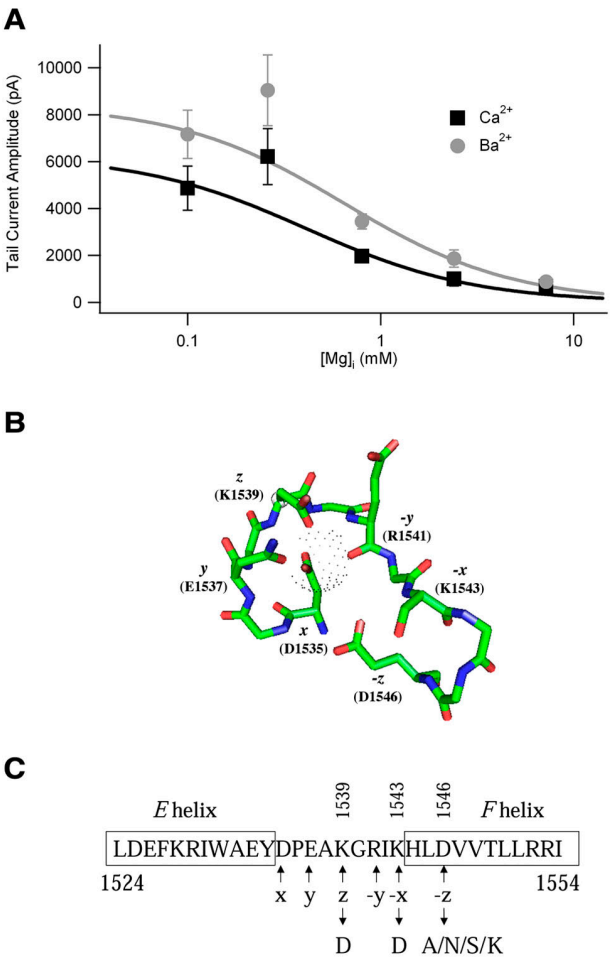

Figure 2. The COOH-terminal EF-hand motif as a possible Mg^{2+} binding site. (A) Effect of Mg^{2+} on I_{Ba} and I_{Ca} through $Ca_v1.2$ channels. Comparison of Mg_i effects on WT channels using 10 mM Ba^{2+} or 1.8 mM Ca^{2+} as the charge carrier. Plot of mean tail current amplitude following test pulses to +80 mV versus Mg_i concentration. The data were fit using a single binding site model. The fit curves are binding isotherms obtained with a global fitting procedure implemented in Igor Pro assuming a common coefficient for the number of binding sites (Hill coefficient). Using this procedure gave a Hill coefficient of 0.77 with 95% confidence limits of ±0.16 and an apparent K_d value for inhibition by Mg_i of 0.65 mM (WT). (B) EF-hand motif of $Ca_V1.2$. Model of binding of Mg^{2+} to the EF-hand of $Ca_V1.2$ illustrating the ion-coordinating residues in a Mg^{2+}-bound EF-hand using the structure of the COOH-terminal EF hand of Mg^{2+}-calbindin (PDB 1IG5) with the $Ca_V1.2$ amino acid residues substituted on it. Amino acid side chain oxygens serve as direct ligands of the bound Mg^{2+} for the positions x, y, z, *and* −z. The ligand at the −y position is donated by the backbone carbonyl oxygen of R1541, and the ligand at the −x position is the oxygen atom of an H_2O bound to K1543 (not depicted). The Mg^{2+} ion is represented by a dot surface. Sequence numbers identified below each ligand position denote the corresponding residues in $Ca_V1.2$. (C) Amino acid sequence of the EF-hand of $Ca_V1.2$ and the mutations made at each position.

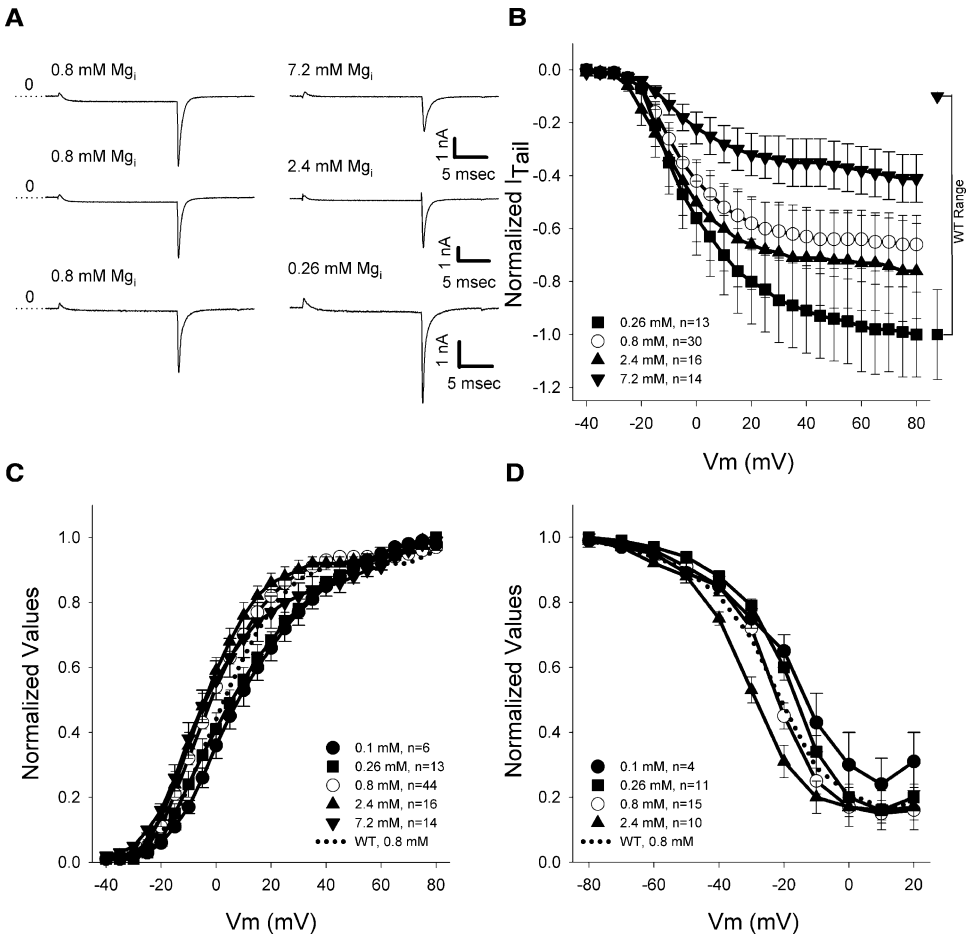

Figure 3. Mg_i modulation of $Ca_V1.2$ channels with EF-hand mutation D1546N. (A) Typical current traces of cells expressing mutant D1546N exposed to a range of Mg_i. The trace at 0.8 mM Mg_i in each pair is from the same series of experiments as the trace at a different Mg_i concentration in the right hand column. (B) Effect of changes in Mg_i on tail current amplitude normalized as in Fig. 1 to the mean I_{tail} for WT at 0.26 mM Mg_i. Bracket illustrates WT Range as in Fig. 1. (C) Effect of Mg_i on voltage dependence of activation measured as in Fig. 1. (D) Effect of Mg_i on the voltage dependence of inactivation measured as in Fig. 1.

bal fit of all of our results with WT and mutant channels (see below).

To determine whether the effect of Mg_i would be observed under physiological conditions, we performed similar experiments with Ca^{2+} (1.8 mM) as charge carrier (Fig. 2 A). Similar to the experiments with Ba^{2+}, we found that peak Ca^{2+} currents were significantly decreased as a function of Mg_i, and the inhibition could be approximated by a single-site binding isotherm with an apparent K_d value of 0.41 mM (Fig. 2 A). As for Ba^{2+} currents, we also observed shifts in the voltage dependence of activation and inactivation of Ca^{2+} currents. Lower Mg_i (0.26 and 0.1 mM) positively shifted the voltage dependence of activation by ~10 mV (6.6 ± 0.7 mV, $n = 10$, at 0.26 mM and 7.1 ± 0.8 mV, $n = 11$, at 0.1 mM vs. −3.1 ± 0.4 mV, $n = 35$, at 0.8 mM, $P < 0.001$), while higher Mg_i (7.2 mM) negatively shifted the voltage dependence of activation by ~8 mV (−11.3 ± 0.3 mV, $n = 9$, vs. −3.1 ± 0.4 mV, $n = 35$, $P < 0.001$). As activation was complete at +30 mV, the measurements of peak Ca^{2+} currents (Fig. 2 A) were unaffected by the changes in voltage dependence. Because Ca^{2+} binds with far higher affinity to the pore of $Ca_V1.2$ channels than Ba^{2+}, the similarity of apparent K_d values for inhibition of Ca^{2+} and Ba^{2+} currents suggests that the effects of Mg_i are not mediated by competitive binding to the Ca^{2+} coordination sites in the ion selectivity filter of the pore.

Effects of Neutralization of a Negative Charge at Position 1546 in the COOH-terminal EF-hand

To determine whether interaction of Mg_i with the COOH-terminal EF-hand (Fig. 2, B and C) was responsible for mediating the electrophysiological effects on $Ca_V1.2$ channels, we tested the mutations of D1546 (−z position) to A, N, or S, which are predicted to reduce affinity for Mg_i (da Silva and Reinach, 1991; Kawasaki and Kretsinger, 1994; da Silva et al., 1995). Compared with WT $Ca_V1.2$ channels, increasing Mg_i had a much smaller effect on the peak tail current amplitude of D1546A/N/S mutant channels, as illustrated in Fig. 3 A for D1546N. In the presence of 0.8 mM Mg_i, the tail current activated at −25 mV, progressively increased with more depolarized test potential up to +20 mV and reached a plateau at more positive test potentials as for WT (Fig. 3 B). However, in contrast to WT $Ca_V1.2$ channels (Fig. 3 B, WT range), changes of Mg_i from 7.2 to 0.26 mM had much smaller effects on peak tail currents

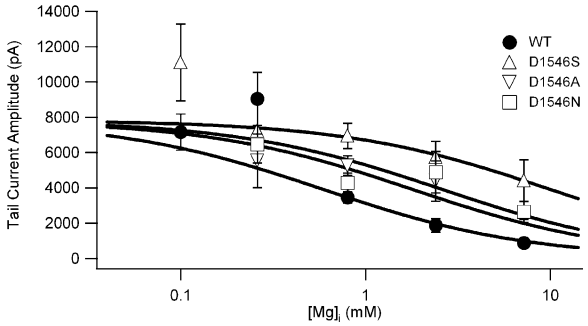

Figure 4. Effects of mutations D1546A/N/S in the EF-hand of $Ca_V1.2$ on sensitivity to Mg^{2+}. Modulation of I_{Ba} through WT and mutant $Ca_V1.2$ channels by Mg^{2+}. The fit curves are binding isotherms obtained with a global fitting procedure implemented in Igor Pro and applied to the effects of Mg^{2+} on all WT and mutant channels. It assumed a common asymptote at 0 Mg_i and a common coefficient for the number of binding sites (Hill coefficient). Using this procedure gave a Hill coefficient of 0.77 with 95% confidence limits of ±0.16. Apparent K_d values for inhibition by Mg_i were 9.9 mM (D1546S), 2.6 mM (D1546A), 1.8 mM (D1546N). The assumption of a common asymptote was tested by fitting the data individually using the common Hill coefficient (0.77) and comparing the individual extrapolated ordinate asymptotes. No statistically significant difference in extrapolated maximum current at Mg_i = 0 was observed, consistent with the conclusion that all mutants were expressed similarly to WT.

of the D1546A/N/S mutants, as illustrated in Fig. 3 B for D1546N. These results are consistent with reduced affinity for binding of Mg_i to the altered EF-hands of these mutants.

In this group of mutants, the voltage dependence of activation was similar to WT at 0.8 mM Mg_i. However, reduction to 0.26 mM Mg_i caused a positive shift in the conductance–voltage relationship, while increase to 2.4 mM Mg_i caused a negative shift for D1546A/N/S (Fig. 3 C, D1546N). The voltage dependence of inactivation of D1546A/N/S was indistinguishable from WT, and included the shift of approximately −5 mV in the voltage dependence of inactivation at 2.4 mM Mg_i (Fig. 3 D, D1546N).

As for WT $Ca_v1.2$ channels, the changes in voltage dependence of activation and inactivation caused by the mutations were small, and peak Ba^{2+} currents reached a plateau at the test pulses more positive than 30 mV. We plotted the mean tail currents for several cells expressing each mutant versus the concentration of Mg_i in order to estimate the apparent K_d for reduction of peak Ba^{2+} currents by Mg_i (Fig. 4). These results show that the K_d increased to ∼1.8 mM for D1546N, 2.6 mM for D1546A, and 9.9 mM for D1546S, ∼3- to 16.5-fold higher than WT. However, the limited range of Mg_i concentration accessible for investigation prevented us from defining more precise K_d values for the mutants.

Effects of Substitution of a Positive Charge for D1546 in the COOH-terminal EF-hand

To further disrupt the electrostatic interaction between Mg_i and the EF-hand, we introduced a positive charge at position 1546 (D1546K, −z position), and the electrophysiological properties of this mutant and effects of Mg_i on its function were tested. Substitution of the positively charged K for a negatively charged D that directly interacts with the bound cation in the EF-hand would be expected to completely prevent binding of Mg^{2+} and other divalent cations because of charge–charge repulsion. As for WT channels, in the presence of 0.8 mM Mg_i, the tail current conducted by mutant D1546K was detectable at −25 mV, progressively increased with more depolarized test potential up to +20 mV, and reached a plateau at more positive test potentials (Fig. 5, A and B). However, in contrast to WT $Ca_V1.2$ and D1546A/N/S channels, changes of Mg_i from 7.2 to 0.26 mM had much smaller effects on peak tail currents of the D1546K mutants (WT range; Fig. 5 B). These results are consistent with reduced affinity for binding of Mg_i to the altered EF-hand of this mutant.

The voltage dependence of activation of this mutant was negatively shifted compared with WT at 0.8 mM Mg_i. Reduced Mg_i (0.1 mM) caused a positive shift in the conductance–voltage relationship similar to WT (Fig. 5 C); however, in contrast to WT $Ca_V1.2$ channels, higher Mg_i (7.2 mM) did not negatively shift the voltage dependence of activation (Fig. 5 C). The voltage dependence of inactivation was modified by Mg_i similarly to WT (Fig. 5 D).

Compared with the WT $Ca_V1.2$ channels, Mg_i had a much smaller effect on the peak tail current amplitude of D1546K mutant channel across the full range that we were able to study (Fig. 6). The peak tail currents recorded from 0.26 mM Mg_i to 7.2 mM Mg_i were fit by a straight line with zero slope (Fig. 6), and a single binding site isotherm did not give an improved fit (not presented). These results indicate that the effect of Mg_i is completely lost in this charge-reversal EF-hand mutant over the physiologically relevant concentration range.

Effect of Addition of a Negative Charge at Position 1543 in the COOH-terminal EF-hand

To determine whether the affinity of Mg_i for the COOH-terminal EF-hand of $Ca_V1.2$ could be increased by the addition of a negative charge, D was introduced at two ligand coordination positions, K1543 (−x position, Fig. 2, B and C) and K1539 (z position, see below), and the electrophysiological properties and effects of Mg_i were tested. Mutation K1543D increased the effects of Mg_i. Increasing Mg_i from 0.8 to 2.4 mM led to a substantial reduction of normalized peak tail current amplitude (Fig. 7, A and B). Moreover, reducing Mg_i to 0.26 mM caused a much smaller increase in

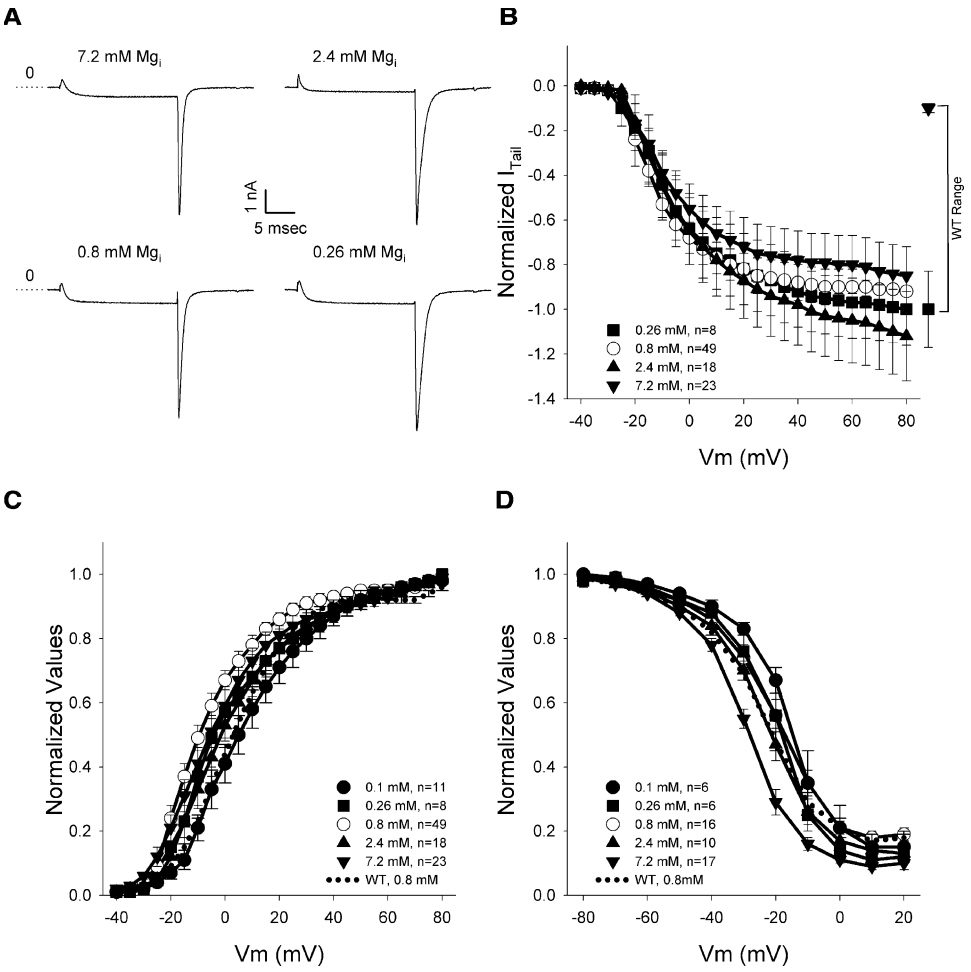

Figure 5. Mg_i modulation of $Ca_V1.2$ channels with the EF-hand mutation D1546K. (A) Typical current traces of cells expressing mutant D1546K exposed to a range of Mg_i. (B) Effect of changes in Mg_i on tail current amplitude normalized as in Fig. 1 to the mean I_{tail} for WT at 0.26 mM Mg_i. Bracket illustrates WT Range as in Fig. 1. (C) Effect of Mg_i on voltage dependence of activation measured as in Fig. 1. (D) Effect of Mg_i on the voltage dependence of inactivation measured as in Fig. 1.

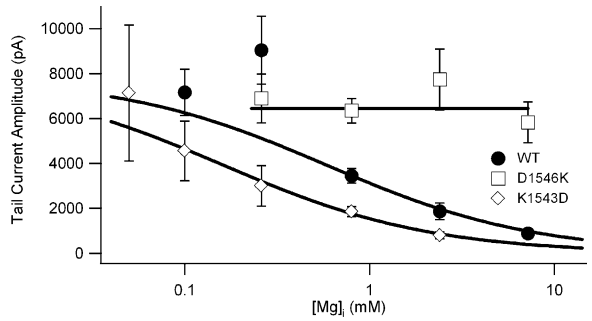

Figure 6. Effects of mutations D1546K and K1543D in the EF-hand of $Ca_V1.2$ on sensitivity to Mg^{2+}. Modulation of I_{Ba} through WT and mutant $Ca_V1.2$ channels by Mg^{2+}. The fit curves are binding isotherms obtained with a global fitting procedure implemented in Igor Pro as described in the legend to Fig. 4. The apparent K_d value for inhibition by Mg_i was 0.16 mM for K1543D. The fit to the D1546K data was not significantly better than the fit to a horizontal straight line, so the horizontal line is plotted. The assumption of a common asymptote was tested by fitting the data individually using the common Hill coefficient (0.77) and comparing the individual extrapolated ordinate asymptotes. No statistically significant difference in extrapolated maximum current at $Mg_i = 0$ was observed, consistent with the conclusion that all mutants were expressed similarly to WT.

tail currents than for WT, while further reduction to 0.1 mM Mg_i gave a more substantial increase in peak tail currents. These results are consistent with increased affinity for inhibition by Mg_i (see below).

In contrast to the D1546A/N/S mutants, the voltage dependence of activation of K1543D was shifted −6 mV compared with WT (Fig. 7 C). Increasing Mg_i concentration to 2.4 mM did not cause a further shift in the activation relationship, while decreasing Mg_i positively shifted activation (Fig. 7 C). The voltage dependence of inactivation was unchanged from WT for K1543D at 0.8 mM Mg_i, but 2.4 mM Mg_i negatively shifted the voltage dependence of inactivation as for WT $Ca_V1.2$ channels (Fig. 7 D). Lower Mg_i ($\leq$0.26 mM) caused voltage-dependent inactivation to be strikingly incomplete at positive test pulse potentials (Fig. 7 D).

The smaller inhibition by increasing Mg_i compared with WT coupled with the larger increase in I_{Ba} with decreasing Mg_i indicate increased apparent affinity for inhibition of peak currents by Mg^{2+}. Because WT and all four mutants substituting A, N, S, and K at position 1546 give a similar extrapolated peak I_{Ba} when fit to a single binding site isotherm (Figs. 4 and 6), we have

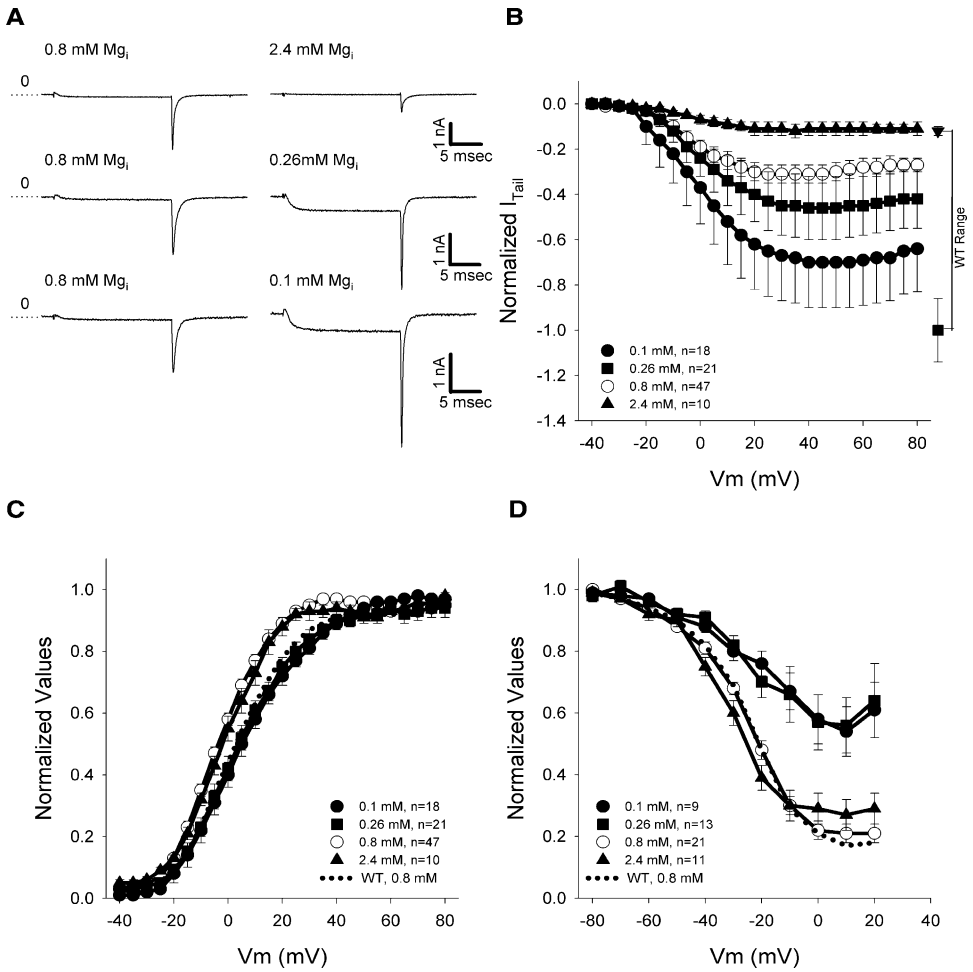

Figure 7. Mg_i modulation of $Ca_V1.2$ channels with the EF-hand mutation K1543D. (A) Typical current traces of cells expressing $Ca_V1.2$ EF-hand mutant K1543D exposed to a range of Mg_i. (B) Effect of Mg_i on tail current amplitude normalized as in Fig. 1 to the mean I_{tail} for WT at 0.1 mM Mg_i. Bracket illustrates WT Range as in Fig. 1. (C) Effect of Mg_i on the voltage dependence of activation measured as in Fig. 1. (D) Effect of Mg_i on the voltage dependence of inactivation measured as in Fig. 1.

plotted the results for K1543D in a similar manner (Fig. 6). The experimental results are well fit by a single binding site model with an apparent K_d of 0.16 mM for Mg_i and a similar maximum I_{Ba}. Thus, these results are consistent with ~4.1-fold higher affinity for inhibition of peak $Ca_V1.2$ currents by Mg_i in the K1543D mutant. Alternative interpretations of these results are considered in DISCUSSION.

A Single Site Model for Mg^{2+} Inhibition

To test the significance of the single binding site model we have used to fit our results (Figs. 4 and 6), we used a global fit protocol to analyze simultaneously the fit of all of our results for inhibition of WT and mutant $Ca_V1.2$ channels by Mg_i to a binding isotherm with a variable Hill slope, constraining that value to be the same for all of the experimental results. The resulting fit yielded an estimate of Hill slope of 0.77 with 95% confidence limits of ±0.16. These results are consistent with a single-binding-site model for Mg_i inhibition and are significantly different from a two-binding-site model. This analysis validates use of a single binding site model for inhibition of $Ca_V1.2$ channels by Mg_i and provides support for our estimates of apparent K_d values based on a single binding site model.

Effects of Addition of a Negative Charge at Position 1539 in the COOH-terminal EF-hand

In contrast to K1543D, changes in Mg_i from 0.1 to 2.4 mM did not have a concentration-dependent effect on peak tail currents of K1539D, as if the effect of Mg_i was saturated at these concentrations (Fig. 8 A). Further reduction in Mg_i to 0.05 mM significantly increased peak tail currents, indicating that Mg_i inhibition of this mutant was complete at 0.1 mM and above (Fig. 8 A).

The voltage dependence of activation of K1539D was shifted +10 mV from WT at 0.8 mM Mg_i. Increased Mg_i caused a negative shift (−6 mV), whereas decreased Mg_i caused a positive shift (+11 mV) of the voltage dependence of activation (Fig. 8 B). Changes of Mg_i did not alter the voltage dependence of inactivation substantially, but reduced Mg_i (0.1 mM) caused strikingly incomplete inactivation at positive membrane potentials as for K1543D (Fig. 8 C).

Although K1539D has altered voltage dependence of activation and inactivation, we were able to accurately

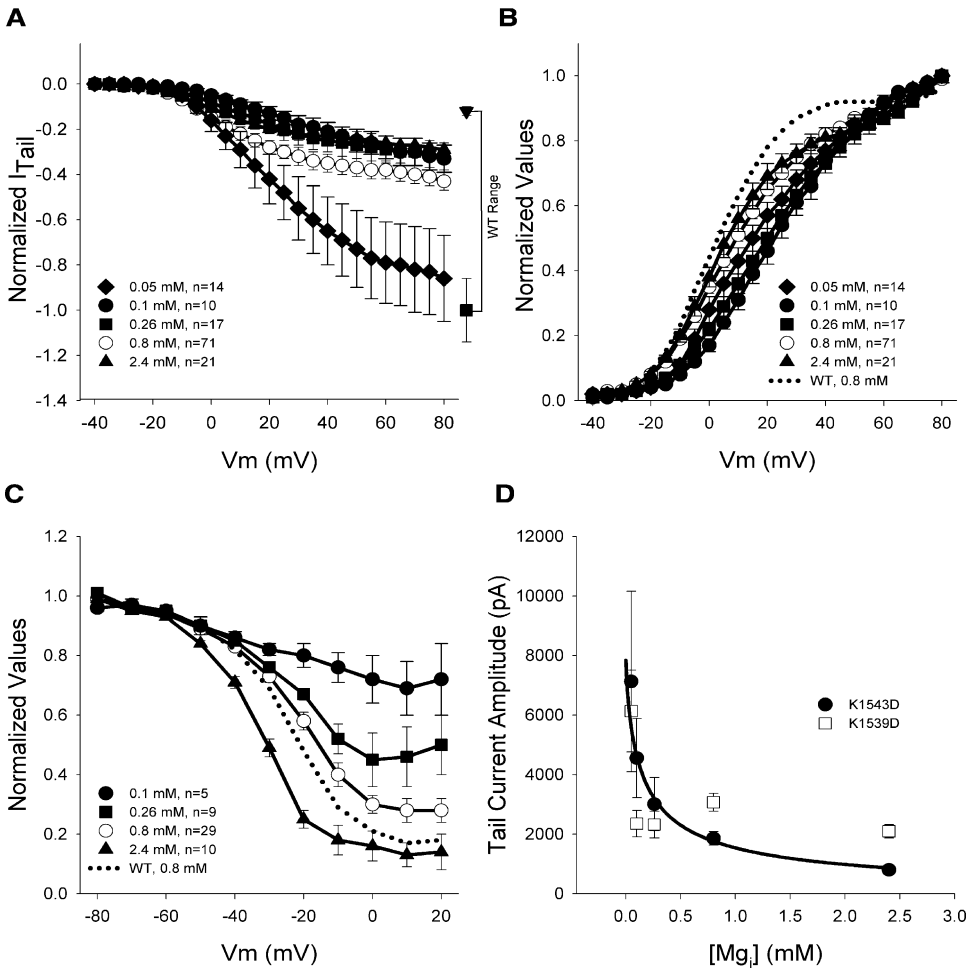

Figure 8. Mg_i modulation of $Ca_V1.2$ channels with the EF-hand mutation K1539D. (A) Effect of Mg_i on tail current amplitude normalized as in Fig. 1 to the mean I_{tail} for WT at 0.1 mM Mg_i. Bracket illustrates WT Range as in Fig. 1. (B) Effect of Mg_i on the voltage dependence of activation measured as in Fig. 1. (C) Effect of Mg_i on the voltage dependence of inactivation measured as in Fig. 1. (D) Concentration dependence of Mg_i modulation of tail current amplitude in K1543D and K1539D. The solid line is the fit of a single binding site model to the K1543D data.

measure the plateau of peak Ba^{2+} tail currents following test pulses to potentials more positive than 30 mV. However, unlike the results with other mutants, these results did not fit a single binding site isotherm well. Comparison of these values to the binding isotherm for mutant K1543D (Fig. 8 D) suggests the possibility that K1539D does indeed have increased apparent affinity for inhibition of peak current by Mg_i, comparable to K1543D, but K1539D also has a reduced maximum extent of inhibition leading to a plateau at ~19% of maximum current at $Mg_i > 0.1$ mM.

DISCUSSION

Mg^{2+} Concentrations Change in Cardiovascular Diseases

Intracellular Mg^{2+} is primarily bound, and free Mg^{2+} levels are altered in response to changes in the levels of macromolecular Mg^{2+} binding sites and soluble Mg^{2+} chelators such as nucleotides. The transport mechanisms that allow Mg^{2+} to cross the plasma membrane and control the levels of intracellular Mg^{2+} in order to maintain homeostasis are poorly understood. However, given the high concentration of Mg-ATP in cells, it may be expected that conditions that substantially alter ATP levels would also alter free Mg_i. Consistent with this expectation, free Mg_i in cardiac myocytes increases from 0.6–0.7 mM to 2.1–2.3 mM in parallel with the decrease in ATP levels during myocardial ischemia in rat heart (Murphy et al., 1989; Headrick and Willis, 1991). Free Mg_i also increases during transient decreases in pH (Freudenrich et al., 1992), which may contribute to the increase observed in ischemia as intracellular H^+ concentration rises due to lactic acid production. Increased extracellular Mg^{2+} is cardioprotective for patients during episodes of ischemia (McCully and Levitsky, 1997). Many mechanisms may contribute to this cardioprotective effect, but inhibition of Ca^{2+} entry via $Ca_V1.2$ channels would be a likely candidate for a major role in cardioprotection because of the large L-type Ca^{2+} currents in myocytes and the high sensitivity of myocytes to the cytotoxic effects of excess cytosolic Ca^{2+}.

In contrast to the increase in free Mg_i during acute episodes of myocardial ischemia, chronic experimental heart failure in dogs is accompanied by a decrease in

intracellular free Mg^{2+} from 1.06 to 0.49 mM (Haigney et al., 1998). The mechanism of this prolonged effect on free Mg_i is unknown, but it is associated with altered ventricular repolarization, which may predispose to dangerous arrhythmias. Together with the results on myocardial ischemia, these results on heart failure support the conclusion that there are substantial variations in myocardial free Mg_i during pathological conditions.

Intracellular Mg^{2+} Inhibits Transfected $Ca_v1.2$ Channels

White and Hartzell (1988) showed that exposure of cardiac myocytes to increasing concentrations of intracellular Mg^{2+} (0.3–3 mM) reduces the L-type Ca^{2+} current density. The reduction of L-type Ca^{2+} current in isolated cardiac myocyte preparation has been reproduced by many other laboratories (Agus et al., 1989; Yamaoka and Seyama, 1996; Pelzer et al., 2001; Wang et al., 2004). Here we show that this effect is also observed for cloned $Ca_v1.2$ channels expressed in human embryonic kidney tsA-201 cells. These results indicate that the inhibitory effect of Mg_i on $Ca_v1.2$ channels does not require proteins that are specific to cardiac cells and provide a model system for analysis of the molecular mechanism of the effect of Mg_i.

Mg_i Acts through the COOH-terminal EF-hand to Inhibit $Ca_v1.2$ Channels

The mechanism responsible for the effects of Mg_i on Ca^{2+} currents in cardiac cells has been controversial. Some reports support direct interaction of Mg_i with the cardiac Ca^{2+} channel (Kuo and Hess, 1993; Yamaoka and Seyama, 1996) while others support an indirect mode of interaction for Mg_i via modification of the activities of protein kinases or phosphoprotein phosphatases (McGowan and Cohen, 1988; Pelzer et al., 2001; Wang et al., 2004). By analysis of the effects of mutations in a potential Mg^{2+}-binding EF-hand motif, our experiments support direct action of Mg^{2+} on the Ca^{2+} channel protein that reduces peak L-type Ba^{2+} currents through the Ca^{2+} channel by binding to the COOH-terminal EF-hand of $Ca_V1.2$ channels.

The ligand-binding amino acid residues in EF-hands are well known (Kawasaki and Kretsinger, 1994), allowing design of mutations that are known to affect divalent cation binding directly and specifically in other structurally defined, EF-hand–containing proteins. We found that mutations of ion-coordinating amino acids of the COOH-terminal EF-hand lead to alterations in Mg_i sensitivity. Mutations at position 1546 (D1546A/N/S) that are predicted to reduce Mg^{2+} affinity caused a substantial reduction in the sensitivity of Mg_i inhibition, consistent with 4.1- to 16.5-fold increase in the apparent K_d for Mg^{2+} binding. In addition, introducing a positive charge at that position in mutant D1546K completely removed Mg_i sensitivity over the concentration range that we tested. Our results are in agreement with previous experimental observations showing that D at the $-z$ position (here D1546) of EF-hand ion-coordination binding sites is a key amino acid residue for the binding of Mg_i to EF-hand motifs (Kawasaki and Kretsinger, 1994; da Silva et al., 1995; Yang et al., 2002).

The complementary mutation K1543D that is predicted to increase affinity for Mg_i caused a substantial increase in sensitivity to Mg_i inhibition, consistent with 4.1-fold reduction in apparent K_d for Mg^{2+} inhibition. Moreover, our results with the complementary mutation K1539D also suggest an increase in apparent affinity, although we could not quantitate the change because the concentration dependence did not conform to a single binding isotherm. Altogether, these results support a model in which Mg_i directly interacts with the COOH-terminal EF-hand of the $Ca_V1.2$ channel to reduce current amplitude.

Because there is only a single EF-hand in the $Ca_V1.2$ channel, effects of Mg^{2+} acting through that site would be expected to conform to a single binding-site model. Using a global fitting protocol, we found that our results for WT, D1546A/N/S/K, and K1543D mutants could be successfully fit to a single binding site model with a Hill coefficient of 0.77 and 95% confidence limits of 0.16. This fit was significantly better than a fit to a two-site model. Therefore, our results support the conclusion that binding of a single Mg^{2+} ion to the COOH-terminal of EF-hand $Ca_V1.2$ channels substantially reduces peak Ba^{2+} or Ca^{2+} currents.

Our global fitting protocol also allows us to address the possibility that altered expression levels of the mutants compared with WT had a major effect on our results. We extrapolated the inhibition curves to $Mg_i = 0$ to eliminate the different effects of Mg_i on WT and mutants. This extrapolation was made without any normalization of the data at different Mg_i concentrations. Comparison of these extrapolated values showed that none differed significantly from WT ($P > 0.5$), providing further support for our estimates of apparent Kd values for inhibition of $Ca_V1.2$ channels by Mg^{2+} binding to the EF-hand.

Comparison to Previous Work on Regulation of $Ca_V1.2$ Channels by Mg^{2+} and Protein Phosphorylation

The findings reported here are in agreement with those of other groups who concluded that the ion-coordinating residues of this EF-hand do not serve as a Ca^{2+} sensor for Ca^{2+}-dependent inactivation of $Ca_V1.2$ channels (Zhou et al., 1997; Bernatchez et al., 1998; Peterson et al., 2000). Based on mutagenesis analysis of structural residues that do not participate in ion coordination in the EF-hand, Peterson et al. (2000) proposed that the F-helix (Fig. 2 B) serves as a transducer in mediating Ca^{2+}-dependent inactivation. If this idea is correct, Mg^{2+} binding to the EF-hand

may indirectly alter Ca^{2+}-dependent inactivation. Further experiments will be required to assess this possibility. However, careful design and interpretation of such experiments will be necessary because we have found that Mg^{2+} binding to the COOH-terminal EF-hand substantially increases Ca^{2+}-independent, voltage-dependent inactivation, which would complicate measurements of effects on Ca^{2+}-dependent inactivation (Brunet et al., 2005).

The COOH-terminal domain of $Ca_v1.2$ channels has previously been established as an important locus for regulation by β-adrenergic receptor-stimulated phosphorylation by cAMP-dependent protein kinase and by Ca^{2+}/calmodulin binding (Catterall, 2000). Our results add Mg_i to the growing list of regulators that control Ca^{2+} channel activity through interaction with the COOH-terminal domain.

Previous work (Kuo and Hess, 1993) has shown that Mg_i blocks unitary L-type inward currents through single Ca^{2+} channels in cultured pheochromocytoma cells, suggesting that direct pore block is an alternative mechanism through which Mg_i could reduce peak Ba^{2+} currents in our experiments. However, the K_d for pore block in those experiments (Kuo and Hess, 1993) varied from ∼40 mM at −70 mV to 8 mM at +20 mV. In contrast, the block of $Ca_v1.2$ channels we observe here has a K_d of 0.7 mM and the K_d does not vary significantly between −20 and +80 mV. In addition, we found that block of Ca^{2+} and Ba^{2+} currents had approximately the same apparent K_d for Mg_i, which is inconsistent with competitive block of the pore because the ion coordination site in the pore has much higher affinity for Ca^{2+} than Ba^{2+}. Therefore, direct pore block by Mg_i is unlikely to contribute significantly to our measurements and also appears unlikely to occur under physiological conditions in cardiac myocytes.

Although our results establish an important role for direct binding of Mg_i to the COOH-terminal EF-hand in modulation of L-type Ca^{2+} currents conducted by $Ca_v1.2$ channels, they do not exclude additional important effects of Mg_i that may be mediated indirectly through changes in the activities of protein kinases or phosphoprotein phosphatases (White and Hartzell, 1988; Agus et al., 1989; Yamaoka and Seyama, 1996; Pelzer et al., 2001; Wang et al., 2004). The effects of kinases and phosphatases might be more pronounced in cardiac myocytes, where their concentrations are higher and specific targeting to Ca^{2+} channels by anchoring proteins or scaffolding proteins may enhance their effects. Thus, it will be important to examine the range of functional effects in cardiac myocytes that can be ascribed to the direct actions of Mg_i through the EF-hand of Ca^{2+} channels as described here and to determine whether there are additional regulatory effects that are related to modification of the enzymatic activities of kinases and phosphatases.

Effects of Mg^{2+} on the Voltage Dependence of Activation and Inactivation of $Ca_v1.2$ Channels

Significant shifts in the voltage dependence of activation and inactivation were observed at high (7.2 mM) and low (≤0.26 mM) Mg_i concentrations. Most of these effects likely result from screening of negative charges on the intracellular surface of the Ca^{2+} channel protein or surrounding membrane because increasing Mg_i causes negative shifts of voltage dependence in most cases, consistent with an intracellular charge-screening mechanism. In contrast to these charge-screening effects, at low Mg_i (0.26 and 0.1 mM Mg_i) the extent of voltage-dependent inactivation at positive membrane potentials was substantially reduced, especially in the K1539D and K1543D mutants. These results suggest that the introduction of a negative charge in the ion-coordination site in the COOH-terminal EF-hand alters voltage-dependent inactivation through an allosteric effect on the inactivation gating process. Binding of Mg^{2+} to this EF-hand in WT $Ca_V1.2$ channels may be a necessary structural element for normal voltage-dependent inactivation.

Potential Physiological Role of Inhibition of $Ca_v1.2$ Channels by Mg^{2+} Binding

What is the physiological role of inhibition of cardiac Ca^{2+} channels by Mg^{2+} binding? We propose that Mg_i modulation of $Ca_V1.2$ may be an important part of a cardiac stress response to reduced energy metabolism designed to maintain Ca^{2+} homeostasis. In ischemic stress, rising Mg_i as a result of increased Mg-ATP hydrolysis is sensed by at least three key proteins important for EC-coupling: the $Ca_v1.2$ channel, the type-2 ryanodine-sensitive Ca^{2+} release channel RYR2, and the sarcoplasmic reticulum Ca^{2+} pump SERCA2a. Elevated Mg_i inhibits $Ca_v1.2$ (White and Hartzell, 1988, 1989; Hartzell and White, 1989; Agus et al., 1989; Yamaoka and Seyama, 1996; Pelzer et al., 2001; Wang et al., 2004) and RYR2 (Copello et al., 2002) but stimulates SERCA2a (Mahey and Katz, 1990). Thus, the overall effect of increased Mg_i would be to maintain intracellular Ca^{2+} at a low level. The Mg_i increase is terminated when ATP production is reestablished and buffers Mg_i back to pre-ischemic levels. Therefore, we propose that by sensing intracellular Mg_i the $Ca_v1.2$ channel is able to monitor the metabolic status of the cardiac myocyte, adjust the amount of trigger Ca^{2+} that enters the cell, and ultimately fine tune the contractile function and cardiac output of the heart under conditions of stress.

In addition to the effects of changes in Mg_i levels during ischemic stress, Lehnart et al. (2004) described several mutations of the RYR2 that have reduced Mg_i sensitivity. Interestingly, these mutations are associated with catecholaminergic polymorphic ventricular tachycardia (CPVT) (Priori et al., 2002), in which patients

have arrhythmic episodes and sudden death mainly during periods of exercise-induced stress. Evidently, the decreased Mg_i sensitivity of RYR2 may generate arrhythmias in response to rises in Ca_i during exercise-induced stress, in addition to the altered inhibitory role of FKBP12.6 (calstabin2), which is also caused by these mutations (Wehrens et al., 2004). Thus, defects in Mg_i homeostasis and/or altered sensitivity of proteins to Mg_i could be associated with negative clinical outcome in patients under conditions of increased stress, including ischemia, exercise, cardiac hypertrophy, and heart failure. Our findings indicate that modulation of $Ca_v1.2$ channels by Mg_i binding to the COOH-terminal EF-hand may contribute to the multiplicity of effects of this crucial intracellular ion in both physiological and pathophysiological states.

We thank Dr. Robert Kretsinger (University of Virginia, Charlottesville, VA) for valuable discussions of the structure and function of EF-hand motifs.

The authors gratefully acknowledge the financial support provided by the National Institutes of Health (P01 HL 44948) to W.A. Catterall and R. Klevit, and a postdoctoral research fellowship from the American Heart Association to S. Brunet.

Olaf S. Andersen served as editor.

Submitted: 20 May 2005
Accepted: 3 August 2005

REFERENCES

Agus, Z.S., E. Kelepouris, I. Dukes, and M. Morad. 1989. Cytosolic magnesium modulates calcium channel activity in mammalian ventricular cells. *Am. J. Physiol.* 256:C452–C455.

Bernatchez, G., D. Talwar, and L. Parent. 1998. Mutations in the EF-hand motif impair the inactivation of barium currents of the cardiac α1C channel. *Biophys. J.* 75:1727–1739.

Bers, D.M., C.W. Patton, and R. Nuccitelli. 1994. A practical guide to the preparation of Ca^{2+} buffers. *Methods Cell Biol.* 40:3–29.

Brunet, S., T. Scheuer, R. Klevit, and W.A. Catterall. 2004. Modulation of $Ca_V1.2$ channels by Mg^{2+} binding to an EF-hand motif in the C-terminal domain. *Biophys. J.* 86:274a.

Brunet, S., T. Scheuer, and W.A. Catterall. 2005. Intracellular magnesium enhances voltage-dependent inactivation of $Ca_V1.2$ by binding to the C-terminal EF-hand. *Biophys. Soc. Abst.* 976-Plat.

Catterall, W.A. 2000. Structure and regulation of voltage-gated Ca^{2+} channels. *Annu. Rev. Cell Dev. Biol.* 16:521–555.

Copello, J.A., S. Barg, A. Sonnleitner, M. Porta, P. Diaz-Sylvester, M. Fill, H. Schindler, and S. Fleischer. 2002. Differential activation by Ca^{2+}, ATP and caffeine of cardiac and skeletal muscle ryanodine receptors after block by Mg^{2+}. *J. Membr. Biol.* 187:51–64.

da Silva, A.C., and F.C. Reinach. 1991. Calcium binding induces conformational changes in muscle regulatory proteins. *Trends Biochem. Sci.* 16:53–57.

da Silva, A.C., J. Kendrick-Jones, and F.C. Reinach. 1995. Determinants of ion specificity on EF-hands sites. Conversion of the Ca^{2+}/Mg^{2+} site of smooth muscle myosin regulatory light chain into a Ca^{2+}-specific site. *J. Biol. Chem.* 270:6773–6778.

De Jongh, K.S., C. Warner, A.A. Colvin, and W.A. Catterall. 1991. Characterisation of the two size forms of the α1 subunit of skeletal L-type calcium channels. *Proc. Natl. Acad. Sci. USA.* 88:10778–10782.

De Jongh, K.S., B.J. Murphy, A.A. Colvin, J.W. Hell, M. Takahashi, and W.A. Catterall. 1996. Specific phosphorylation of a site in the full-length form of the α1 subunit of the cardiac L-type calcium channel by adenosine 3′, 5′-cyclic monophosphate-dependent protein kinase. *Biochemistry.* 35:10392–10402.

de Leon, M., Y. Wang, L. Jones, E. Perez-Reyes, X. Wei, T.W. Soong, T.P. Snutch, and D.T. Yue. 1995. Essential Ca^{2+}-binding motif for Ca^{2+}-sensitive inactivation of L-type Ca^{2+} channels. *Science.* 270: 1502–1506.

Elin, R.J. 1994. Magnesium: the fifth but forgotten electrolyte. *Am. J. Clin. Pathol.* 102:616–622.

Freudenrich, C.C., E. Murphy, L.A. Levy, R.E. London, and M. Lieberman. 1992. Intracellular pH modulates cytosolic free magnesium in cultured chicken heart cells. *Am. J. Physiol.* 262:C1024–C1030.

Haigney, M.C., S. Wei, S. Kaab, E. Griffiths, R. Berger, R. Tunin, D. Kass, W.G. Fisher, B. Silver, and H. Silverman. 1998. Loss of cardiac magnesium in experimental heart failure prolongs and destabilizes repolarization in dogs. *J. Am. Coll. Cardiol.* 31:701–706.

Hartzell, H.C., and R.E. White. 1989. Effects of magnesium on inactivation of the voltage-gated calcium current in cardiac myocytes. *J. Gen. Physiol.* 94:745–767.

Headrick, J.P., and R.J. Willis. 1991. Cytosolic free magnesium in stimulated, hypoxic, and underperfused rat heart. *J. Mol. Cell. Cardiol.* 23:991–999.

Houdusse, A., and C. Cohen. 1996. Structure of the regulatory domain of scallop myosin at 2 Å resolution: implications for regulation. *Structure.* 4:21–32.

Hulme, J.T., T.W. Lin, R.E. Westenbroek, T. Scheuer, and W.A. Catterall. 2003. β-Adrenergic regulation requires direct anchoring of PKA to cardiac $Ca_V1.2$ channels via a leucine zipper interaction with A kinase-anchoring protein 15. *Proc. Natl. Acad. Sci. USA.* 100:13093–13098.

Kawasaki, H., and R.H. Kretsinger. 1994. Calcium-binding proteins. 1: EF-hands. *Protein Profile.* 1:343–517.

Kuo, C.C., and P. Hess. 1993. Block of the L-type Ca^{2+} channel pore by external and internal Mg^{2+} in rat phaeochromocytoma cells. *J. Physiol.* 466:683–706.

Lehnart, S.E., X.H. Wehrens, P.J. Laitinen, S.R. Reiken, S.X. Deng, Z. Cheng, D.W. Landry, K. Kontula, H. Swan, and A.R. Marks. 2004. Sudden death in familial polymorphic ventricular tachycardia associated with calcium release channel (ryanodine receptor) leak. *Circulation.* 109:3208–3214.

Lewit-Bentley, A., and S. Rety. 2000. EF-hand calcium-binding proteins. *Curr. Opin. Struct. Biol.* 10:637–643.

Mahey, R., and S. Katz. 1990. A non-specific Ca^{2+} (or Mg^{2+})-stimulated ATPase in rat heart sarcoplasmic reticulum. *Mol. Cell. Biochem.* 96:175–182.

Margolskee, R.F., B. McHendry-Rinde, and R. Horn. 1993. Panning transfected cells for electrophysiological studies. *Biotechniques.* 15:906–911.

McCully, J.D., and S. Levitsky. 1997. Mechanisms of in vitro cardioprotective action of magnesium on the aging myocardium. *Magnes. Res.* 10:157–168.

McGowan, C.H., and P. Cohen. 1988. Protein phosphatase-2C from rabbit skeletal muscle and liver: an Mg^{2+}-dependent enzyme. *Methods Enzymol.* 159:416–426.

Murphy, E. 2000. Mysteries of magnesium homeostasis. *Circ. Res.* 86:245–248.

Murphy, E., C. Steenbergen, L.A. Levy, B. Raju, and R.E. London. 1989. Cytosolic free magnesium levels in ischemic rat heart. *J. Biol. Chem.* 264:5622–5627.

Pelzer, S., C. La, and D.J. Pelzer. 2001. Phosphorylation-dependent modulation of cardiac calcium current by intracellular free magnesium. *Am. J. Physiol. Heart Circ. Physiol.* 281:H1532–H1544.

Peterson, B.Z., J.S. Lee, J.G. Mulle, Y. Wang, M. de Leon, and D.T. Yue. 1999. Calmodulin is the Ca^{2+} sensor for Ca^{2+}-dependent inactivation of L-type calcium channels. *Neuron*. 22:549–558.

Peterson, B.Z., C.D. DeMaria, J.P. Adelman, and D.T. Yue. 2000. Critical determinants of Ca^{2+} -dependent inactivation within an EF- hand motif of L-type Ca^{2+} channels. *Biophys. J.* 78:1906–1920.

Priori, S.G., N. Napolitano, M. Memmi, B. Colombi, F. Drago, M. Gasparini, L. DeSimone, F. Coltorti, R. Bloise, R. Keegan, et al. 2002. Clinical and molecular characterization of patients with catecholaminergic polymorphic ventricular tachycardia. *Circulation*. 106:69–74.

Tomaselli, G.F., and E. Marban. 1999. Electrophysiological remodeling in hypertrophy and heart failure. *Cardiovasc. Res.* 42:270–283.

Wang, M., M. Tashiro, and J.R. Berlin. 2004. Regulation of L-type calcium current by intracellular magnesium in rat cardiac myocytes. *J. Physiol.* 555:383–396.

Wehrens, X.H., S.E. Lehnart, S.R. Reiken, S.X. Deng, J.A. Vest, D. Cervantes, J. Coromilas, D.W. Landry, and A.R. Marks. 2004. Protection from cardiac arrhythmia through ryanodine receptor-stabilizing protein calstabin2. *Science*. 304:292–296.

Wei, S.K., J.F. Quigley, S.U. Hanlon, B. O'Rourke, and M.C. Haigney. 2002. Cytosolic free magnesium modulates Na/Ca exchange currents in pig myocytes. *Cardiovasc. Res.* 53:334–340.

White, R.E., and H.C. Hartzell. 1988. Effects of intracellular free magnesium on calcium current in isolated cardiac myocytes. *Science*. 239:778–780.

White, R.E., and H.C. Hartzell. 1989. Magnesium ions in cardiac function. Regulator of ion channels and second messengers. *Biochem. Pharmacol.* 38:859–867.

Xu, L., G. Mann, and G. Meissner. 1996. Regulation of cardiac Ca^{2+} release channel (ryanodine receptor) by Ca^{2+}, H^{+}, Mg^{2+}, and adenine nucleotides under normal and simulated ischemic conditions. *Circ. Res.* 79:1100–1109.

Yamaoka, K., and I. Seyama. 1996. Modulation of Ca^{2+} channels by intracellular Mg^{2+} ions and GTP in frog ventricular myocytes. *Pflugers Arch.* 432:433–438.

Yang, W., H.W. Lee, H. Hellinga, and J.J. Yang. 2002. Structural analysis, identification, and design of calcium-binding sites in proteins. *Proteins*. 47:344–356.

Zhou, J., R. Olcese, N.N.F. Qin, F. Noceti, L. Birnbaumer, and E. Stefani. 1997. Feedback inhibition of Ca^{2+} channels by Ca^{2+} depends on short sequence of the C terminus that does not include the Ca^{2+}-binding function of a motif with similarity to Ca^{2+}-binding domains. *Proc. Natl. Acad. Sci. USA*. 94:2301–2305.

Zuhlke, R.D., G.S. Pitt, K. Deisseroth, R.W. Tsien, and H. Reuter. 1999. Calmodulin supports both inactivation and facilitation of L-type calcium channels. *Nature*. 399:159–162.